

Plug-and-Play Design of Current Controllers for Grid-feeding Converters in DC Microgrids

Renke Han¹, *Student Member, IEEE*, Michele Tucci², *Student Member, IEEE*, Raffaele Soloperto³,
Josep M. Guerrero¹, *Fellow, IEEE*, Giancarlo Ferrari-Trecate⁴, *Senior Member, IEEE*

Abstract—In this paper, we address the problem of synthesizing decentralized current controllers for grid-feeding converters of current-controlled distributed generation units (CDGUs) in dc microgrids (MGs). Notably, a plug-and-play (PnP) design procedure is proposed to achieve grid-feeding current tracking while preserving the collective MG stability. Through the presented control scheme, seamless addition/removal of each CDGU to/from the MG is ensured, with no need to update controllers of neighboring CDGUs and to know the information of the MG. At the mathematical level, the set of control coefficients guaranteeing the aforementioned features is explicitly characterized in terms of simple inequalities. The inequality set only depends on the local parameters. Moreover, the proof of the MG closed-loop stability exploits structured Lyapunov functions, the LaSalle invariance theorem and properties of graph Laplacians. Finally, theoretical results are validated by hardware-in-loop simulation tests.

I. INTRODUCTION

With the increasing penetration of renewable energies into modern electric systems, the concept of microgrid (MG) receives increasing attention from both electric industry and academia. A MG is an autonomous electrical network composed of interconnected renewable energy sources (RESes), energy storage systems (ESSes) and different types of loads, which can operate in either grid-connected or islanded mode [1]. To be specific, in ac MGs, power converters can be classified into the grid-forming converter whose main task is to provide voltage support and the grid-feeding converter whose main task is to supply most of the loads [2], and the same classification can also be applied for dc MGs. Meanwhile, during the past decade, dc MGs (which are studied in this paper) have been recognized as more and more attractive due to higher efficiency, more natural interface to many types of RESes and ESSes [3], [4].

For grid-forming converters, several methods, including voltage-current (V-I) droop controller [5], PnP controller [6], [7], are proposed to provide voltage support in dc MGs. The key challenge for V-I droop controller is that the design of

droop coefficients should take into account the specific MG topologies and the value of line impedances [8], [9], [10]. For PnP controllers, the synthesis of a PnP controller requires to solve a convex optimization problem, if unfeasible, the plug-in/out of two corresponding converters must be denied. The proposed controllers mentioned above are only applied for grid-forming converters which are used as the interface for ESSes. However, grid-feeding converters for CDGUs should be also considered when RESes such as photovoltaic (PV) source are interfaced with dc MGs. The current-based PnP controller should be designed for grid-feeding converters to track current reference given by e.g. maximum power point tracking (MPPT) algorithm. Moreover, the current stabilization should also be guaranteed. In [11], a current-based PI primary droop controller is proposed considering the constant current load. In addition, even though several literature [12], [13], [14] considered the problem of energy management operation between RESes and ESSes, to the best of our knowledge, the stability problem of interconnected grid-feeding converters has received little attention from the point view of system level.

In this paper, we propose a PnP scalable procedure for designing local regulators for grid-feeding converters of CDGUs, aiming to achieve offset-free output current tracking. In order to guarantee the current stability of the MG composed by CDGUs, the control coefficients of each controller should fulfill simple inequalities which are only related to the local parameter of CDGUs. Hence, different from the method in [6], [7], no optimization problem need to be solved for designing local regulators; moreover, we show that the design of local controllers capable to stabilize the whole MG is always feasible, independently of the CDGU parameters. Similarly in [7], the proof of closed-loop asymptotic stability of using the proposed controller for CDGUs exploit structured Lyapunov functions, the LaSalle invariance theorem and properties of graph Laplacians. This shows that these tools offer a feasible theoretical framework for analyzing different kinds of MGs equipped with various types of PnP decentralized controllers. Finally, theoretical results are validated by hardware-in-loop (HiL) tests.

II. GRID-FEEDING CONVERTERS OF CURRENT-CONTROLLED DGUS IN DC MICROGRIDS

A. Electrical model of CDGUs

In this subsection, the electrical model for CDGUs is described. The control objective for CDGU is to feed current

¹R. Han and J. M. Guerrero is with Department of Energy Technology, Aalborg University, Aalborg, Denmark {rha, joz}@et.aau.dk

²M. Tucci is with Dipartimento di Ingegneria Industriale e dell'Informazione, Università degli Studi di Pavia, Pavia, Italy michele.tucci02@universitadipavia.it

³R. Soloperto is with Institute of System Theory and Automatic Control, University of Stuttgart, Stuttgart, Germany raffaele.soloperto@ist.uni-stuttgart.de

⁴G. Ferrari-Trecate is with Automatic Control Laboratory, École Polytechnique Fédérale de Lausanne (EPFL), Lausanne, Switzerland giancarlo.ferraritrecate@epfl.ch

This work has received support from the Swiss National Science Foundation under the COFLEX project (grant number 200021-169906)

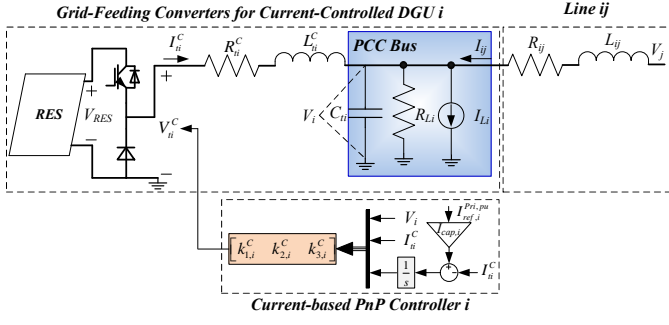


Fig. 1: Electrical scheme of CDGU i and current-based PnP controller.

for the MG through a series RL filter according to the current reference. The electrical scheme of the i -th CDGU is represented within upper part of Fig. 1. It is assumed that loads including both the resistive load and other current disturbance (I_L) are unknown.

Here, an MG composed of N CDGUs is considered. Let us define the set $\mathcal{D}^C = \{1, \dots, N\}$: we call that two CDGUs are neighbors if there is a power line connecting them and denote with $\mathcal{N}_i^C \subset \mathcal{D}^C$ the subset of neighbors of CDGU i . The neighboring relation is symmetric which means $j \in \mathcal{N}_i^C$ implies $i \in \mathcal{N}_j^C$. Furthermore, let $\mathcal{E} = \{(i, j) : i \in \mathcal{D}^C, j \in \mathcal{N}_i^C\}$ collect unordered pairs of indices associated to lines. The topology of the multiple CDGUs is then described by the undirected graph \mathcal{G}_{el} with nodes \mathcal{D}^C and edges \mathcal{E} . From Fig. 1, by applying Kirchoff's voltage and current laws, and exploiting QSL approximation of power lines [6], [15], the model of CDGU i is obtained

$$\text{CDGU } i : \begin{cases} \frac{dV_i}{dt} = \frac{1}{C_{ti}} I_{ti}^C + \sum_{j \in \mathcal{N}_i^C} \left(\frac{V_j}{C_{ti} R_{ij}} - \frac{V_i}{C_{ti} R_{ij}} \right) \\ \quad - \frac{1}{C_{ti}} (I_{Li} + \frac{V_i}{R_{Li}}) \\ \frac{dI_{ti}^C}{dt} = -\frac{1}{L_{ti}^C} V_i - \frac{R_{ti}^C}{L_{ti}^C} I_{ti}^C + \frac{1}{L_{ti}^C} V_{ti}^C \end{cases} \quad (1)$$

where variables V_i , I_{ti}^C , are the i -th PCC voltage and filter current, respectively, V_{ti}^C represents the command to the converter, and R_{ti}^C , L_{ti}^C and C_{ti} represent the electrical parameters of converters. The above description can also be illustrated in Fig. 1. Moreover, V_j is the voltage at the PCC of each neighboring CDGU $j \in \mathcal{N}_i^C$ and R_{ij} is the resistance of the power line connecting CDGUs i and j .

Remark 1: In practical applications, grid-feeding converters need the voltage support from grid-forming converters at the PCC point in the system [2], [3]. In this paper, we focus on the design of current controllers for grid-feeding converters, and analyze the stability of interconnected CDGUs only. Thus, it is assumed that voltages at the PCC points have already been supported by the grid-forming devices. This feature can be guaranteed, for example, by equipping grid-forming converters with PnP decentralized voltage regulators (see [7]).

B. State-space model of multiple CDGUs

Dynamics (1) provides the state-space equations:

$$\Sigma_{[i]}^{CDGU} : \begin{cases} \dot{x}_{[i]}^C(t) = A_{ii}^C x_{[i]}^C(t) + B_i^C u_{[i]}^C(t) + M_i^C d_{[i]}^C(t) \\ \quad + \xi_{[i]}^C(t) + A_{load,i}^C x_{[i]}^C(t) \\ z_{[i]}^C(t) = H_i^C x_{[i]}^C(t) \end{cases}$$

where $x_{[i]}^C = [V_i, I_{ti}^C]^T$ is the state, $u_{[i]}^C = V_{ti}^C$ the control input, $d_{[i]}^C = I_{Li}^C$ the exogenous input including different current loads and $z_{[i]}^C = I_{ti}^C$ the controlled variable of the system. The term $\xi_{[i]}^C = \sum_{j \in \mathcal{N}_i^C} A_{ij}^C (x_{[j]}^C - x_{[i]}^C)$ accounts for the coupling with each CDGU $j \in \mathcal{N}_i^C$ and the term $A_{load,i}^C$ accounts for the resistive load for each CDGU. The matrices of $\Sigma_{[i]}^{CDGU}$ are obtained from (1) as:

$$A_{ii}^C = \begin{bmatrix} 0 & \frac{1}{C_{ti}} \\ -\frac{1}{L_{ti}^C} & -\frac{R_{ti}^C}{L_{ti}^C} \end{bmatrix}, A_{load,i}^C = \begin{bmatrix} -\frac{1}{R_{Li}^C C_{ti}} & 0 \\ 0 & 0 \end{bmatrix}, B_i^C = \begin{bmatrix} 0 \\ \frac{1}{L_{ti}^C} \end{bmatrix}$$

$$A_{ij}^C = \begin{bmatrix} \frac{1}{R_{ij} C_{ti}} & 0 \\ 0 & 0 \end{bmatrix}, M_i^C = \begin{bmatrix} -\frac{1}{C_{ti}} \\ 0 \end{bmatrix}, H_i^C = [0 \quad 1],$$

Remark 2: To be emphasized, there are two main differences between the proposed model for CDGU in (1) and the one proposed in [7]. The first one is that the resistive load is considered as part of the load. The second one is that the control variable is changed from voltage in [7] for grid-forming converters to current in (1) for grid-feeding converters.

The overall model with multiple CDGUs is given by

$$\begin{aligned} \dot{\mathbf{x}}^C(t) &= \mathbf{A}^C \mathbf{x}^C(t) + \mathbf{B}^C \mathbf{u}^C(t) + \mathbf{M}^C \mathbf{d}^C(t) \\ \mathbf{z}^C(t) &= \mathbf{H}^C \mathbf{x}^C(t) \end{aligned} \quad (2)$$

where $\mathbf{x}^C = (x_{[1]}^C, \dots, x_{[N]}^C) \in \mathbb{R}^{2N}$, $\mathbf{u}^C = (u_{[1]}^C, \dots, u_{[N]}^C) \in \mathbb{R}^N$, $\mathbf{d}^C = (d_{[1]}^C, \dots, d_{[N]}^C) \in \mathbb{R}^N$, $\mathbf{z}^C = (z_{[1]}^C, \dots, z_{[N]}^C) \in \mathbb{R}^N$. Matrices \mathbf{A}^C , \mathbf{B}^C , \mathbf{M}^C and \mathbf{H}^C are reported in Appendix A of [16].

III. DESIGN OF STABILIZING CURRENT CONTROLLERS

A. Structure of current-based PnP controllers

In order to track with references $\mathbf{z}_{\text{ref}}^C(t)$, when $\mathbf{d}^C(t) = \bar{\mathbf{d}}^C$ is constant, the CDGU model is augmented with integrators [17]. A necessary condition for making error $\mathbf{e}^C(t) = \mathbf{z}_{\text{ref}}^C(t) - \mathbf{z}^C(t)$ equal to zero as $t \rightarrow \infty$, is that, there are equilibrium states and inputs $\bar{\mathbf{x}}^C$ and $\bar{\mathbf{u}}^C$ verifying (2). The existence of these equilibrium points can be shown following the proof of Proposition 1 in [6].

One obtain the integrator dynamics is (as shown in Fig. 1, setting $z_{\text{ref}[i]}^C = I_{\text{ref},i}^{\text{Pri},\text{pu}} \cdot I_{\text{cap},i}$, where $I_{\text{cap},i}$ is the maximum capability of CDGU i and $I_{\text{ref},i}^{\text{Pri},\text{pu}}$ is the p.u. reference value.)

$$\begin{aligned} \dot{v}_{[i]}^C(t) &= e_{[i]}^C(t) = z_{\text{ref}[i]}^C(t) - z_{[i]}^C(t) \\ &= z_{\text{ref}[i]}^C(t) - H_i^C x_{[i]}^C(t), \end{aligned} \quad (3)$$

and hence, the augmented CDGU model is

$$\hat{\Sigma}_{[i]}^{CDGU} : \begin{cases} \dot{\hat{x}}_{[i]}^C(t) = \hat{A}_{ii}^C \hat{x}_{[i]}^C(t) + \hat{B}_i^C u_{[i]}^C(t) + \hat{M}_i^C \hat{d}_{[i]}^C(t) \\ \quad + \hat{\xi}_{[i]}^C(t) + \hat{A}_{load,i}^C \hat{x}_{[i]}^C(t) \\ \dot{z}_{[i]}^C(t) = \hat{H}_i^C \hat{x}_{[i]}^C(t) \end{cases} \quad (4)$$

where $\hat{x}_{[i]}^C = [[x_{[i]}^C]^T, v_{[i]}^C]^T \in \mathbb{R}^3$ is the state, $\hat{d}_{[i]}^C = [d_{[i]}^C, z_{ref,i}^C]^T \in \mathbb{R}^2$ collects the exogenous signals and $\hat{\xi}_{[i]}^C = \sum_{j \in \mathcal{N}_i} \hat{A}_{ij}^C (\hat{x}_{[j]}^C - \hat{x}_{[i]}^C)$. By direct calculation, the matrices appeared in (4) are as follows

$$\hat{A}_{ii}^C = \begin{bmatrix} A_{ii}^C & 0 \\ -H_i^C & 0 \end{bmatrix}, \quad \hat{A}_{ij}^C = \begin{bmatrix} A_{ij}^C & 0 \\ 0 & 0 \end{bmatrix}, \quad \hat{A}_{load,i}^C = \begin{bmatrix} A_{load,i}^C & 0 \\ 0 & 0 \end{bmatrix},$$

$$\hat{B}_i^C = \begin{bmatrix} B_i^C \\ 0 \end{bmatrix}, \quad \hat{M}_i^C = \begin{bmatrix} M_i^C & 0 \\ 0 & 1 \end{bmatrix}, \quad \hat{H}_i^C = [H_i^C \quad 0].$$

Based on Proposition 2 of [6], the pair $(\hat{A}_{ii}^C, \hat{B}_i^C)$ can be proven to be controllable. Hence, system (4) can be stabilized.

Given from (4), the overall augmented system is

$$\begin{cases} \dot{\hat{\mathbf{x}}}^C(t) = \hat{\mathbf{A}}^C \hat{\mathbf{x}}^C(t) + \hat{\mathbf{B}}^C \mathbf{u}^C(t) + \hat{\mathbf{M}}^C \hat{\mathbf{d}}^C(t) \\ \mathbf{z}^C(t) = \hat{\mathbf{H}}^C \hat{\mathbf{x}}^C(t) \end{cases} \quad (5)$$

where $\hat{\mathbf{x}}^C$ and $\hat{\mathbf{d}}^C$ collect variables $\hat{x}_{[i]}^C$ and $\hat{d}_{[i]}^C$ respectively, and matrices $\hat{\mathbf{A}}^C, \hat{\mathbf{B}}^C, \hat{\mathbf{M}}^C$ and $\hat{\mathbf{H}}^C$ are obtained from systems (4).

Now each CDGU $\hat{\Sigma}_{[i]}^{CDGU}$ is equipped with the following state-feedback controller

$$\mathcal{C}_{[i]}^C : \quad u_{[i]}^C(t) = K_i^C \hat{x}_{[i]}^C(t) \quad (6)$$

where $K_i^C = [k_{1,i}^C \ k_{2,i}^C \ k_{3,i}^C] \in \mathbb{R}^{1 \times 3}$.

It turns out that, together with the integral action (3), controllers $\mathcal{C}_{[i]}^C$, define a multivariable PI regulator, see lower part of Fig. 1. In particular, the overall control architecture is decentralized since the computation of $u_{[i]}^C$ requires the state of $\hat{\Sigma}_{[i]}^{CDGU}$ only. In the following, it is shown that structured Lyapunov functions can be used to ensure asymptotic stability of the system with multiple CDGUs with controllers (6).

B. Conditions for stability of the closed-loop multiple CDGUs

Notation. Here, we use $P > 0$ (resp. $P \geq 0$) for indicating the real symmetric matrix P is positive-definite (resp. positive-semidefinite).

As in [7], the design of control gains hinges on the use of separable local Lyapunov function for certifying the closed-loop stability. Indeed, the structure will also allow us to show that local stability implies stability of the whole system. Here after, the candidate Lyapunov function are considered as

$$V_i^C(\hat{x}_{[i]}^C) = [\hat{x}_{[i]}^C]^T P_i^C \hat{x}_{[i]}^C \quad (7)$$

where positive definite matrices $P_i^C \in \mathbb{R}^{3 \times 3}$ has the structure

$$P_i^C = \left[\begin{array}{c|c} \eta_i & \mathbf{0}_{1 \times 2} \\ \hline \mathbf{0}_{2 \times 1} & \mathcal{P}_{22,i}^C \end{array} \right], \quad (8)$$

where $\eta_i > 0$ is a parameter and the entries of $\mathcal{P}_{22,i}^C$ are arbitrary and denoted as

$$\mathcal{P}_{22,i}^C = \begin{bmatrix} p_{22,i}^C & p_{23,i}^C \\ p_{23,i}^C & p_{33,i}^C \end{bmatrix}. \quad (9)$$

We also assume that given a constant parameter common to all CDGUs $\bar{\sigma} > 0$ just for proof process, the parameters η_i in (8) are set as

$$\eta_i = \bar{\sigma} C_{ti} \quad i \in \mathcal{D}^C. \quad (10)$$

In absence of coupling terms $\hat{\xi}_{[i]}^C(t)$, and load terms $\hat{A}_{load,i}^C \hat{x}_{[i]}^C(t)$, one would like to stabilize the closed-loop CDGU

$$\dot{\hat{x}}_{[i]}^C(t) = \underbrace{(\hat{A}_{ii}^C + \hat{B}_i^C K_i^C)}_{F_i^C} \hat{x}_{[i]}^C(t) + \hat{M}_i^C \hat{d}_{[i]}^C(t). \quad (11)$$

By direct calculation, one has

$$F_i^C = \left[\begin{array}{c|cc} 0 & \frac{1}{C_i} & 0 \\ \hline \frac{(k_{1,i}^C - 1)}{L_{ti}^C} & \frac{(k_{2,i}^C - R_{ti}^C)}{L_{ti}^C} & \frac{k_{3,i}^C}{L_{ti}^C} \\ 0 & -1 & 0 \end{array} \right] = \left[\begin{array}{c|c} 0 & \mathcal{F}_{12,i}^C \\ \hline \mathcal{F}_{21,i}^C & \mathcal{F}_{22,i}^C \end{array} \right] \quad (12)$$

From Lyapunov theory, asymptotic stability of (11) can be certified by the existence of a Lyapunov function as shown in (7) and

$$Q_i^C = [F_i^C]^T P_i^C + P_i^C F_i^C \quad (13)$$

is negative definite. Based on (8) and (12), eq. (13) can be rewritten as

$$Q_i^C = \left[\begin{array}{c|c} 0 & [\mathcal{F}_{21,i}^C]^T \mathcal{P}_{22,i}^C + \eta_i \mathcal{F}_{12,i}^C \\ \hline [\mathcal{F}_{12,i}^C]^T \eta_i + \mathcal{P}_{22,i}^C \mathcal{F}_{21,i}^C & [\mathcal{F}_{22,i}^C]^T \mathcal{P}_{22,i}^C + \mathcal{P}_{22,i}^C \mathcal{F}_{22,i}^C \end{array} \right] \quad (14)$$

The next result shows that, Lyapunov theory certifies, at most, marginal stability of (11).

Firstly, we recall the following elementary properties of the positive definite matrix P_i^C and the negative semi-definite matrix Q_i^C .

Proposition 1: [7] If $Q = Q^T \leq 0$ and an element q_{ii} on the diagonal verified $q_{ii} = 0$, then:

- (i) the matrix Q cannot be negative definite;
- (ii) the i -th row and column have zero entries.

Proposition 2: Matrices $P_i^C > 0$ and $Q_i^C \leq 0$ verifying (8) and (14) have the following structure:

$$P_i^C = \left[\begin{array}{c|cc} \eta_i & 0 & 0 \\ \hline 0 & p_{22,i}^C & 0 \\ 0 & 0 & \frac{k_{3,i}^C}{L_{ti}^C} p_{22,i}^C \end{array} \right], \quad (15)$$

$$Q_i^C = \left[\begin{array}{c|cc} 0 & 0 & 0 \\ \hline 0 & 2 \frac{(k_{2,i}^C - R_{ti}^C)}{L_{ti}^C} p_{22,i}^C & 0 \\ 0 & 0 & 0 \end{array} \right].$$

Moreover, for having $P_i^C > 0$, $Q_i^C \leq 0$ and $Q_i^C \neq 0$, the control coefficients must verify

$$\begin{cases} k_{1,i}^C < 1 \\ k_{2,i}^C < R_{ti}^C \\ k_{3,i}^C > 0 \end{cases} \quad (16)$$

Proof: Based on (9) and (12), the upper right block of (14) can be written as

$$\begin{aligned} & [\mathcal{F}_{21,i}^C]^T \mathcal{P}_{22,i}^C + \eta_i \mathcal{F}_{12,i}^C \\ &= \left[\frac{(k_{1,i}^C - 1)}{L_{ti}^C} p_{22,i}^C + \frac{1}{C_{ti}} \eta_i \mid \frac{(k_{1,i}^C - 1)}{L_{ti}^C} p_{23,i}^C \right] \end{aligned} \quad (17)$$

Based on Proposition 1, (17) should be equal to zero vector which means

$$\begin{cases} \frac{(k_{1,i}^C - 1)}{L_{ti}^C} p_{22,i}^C = -\frac{1}{C_{ti}} \eta_i \\ \frac{(k_{1,i}^C - 1)}{L_{ti}^C} p_{23,i}^C = 0 \end{cases} \quad (18a)$$

$$\begin{cases} \frac{(k_{1,i}^C - 1)}{L_{ti}^C} p_{22,i}^C = -\frac{1}{C_{ti}} \eta_i \\ \frac{(k_{1,i}^C - 1)}{L_{ti}^C} p_{23,i}^C = 0 \end{cases} \quad (18b)$$

Because η_i is positive, one has

$$\begin{cases} k_{1,i}^C < 1 \\ p_{23,i}^C = 0 \end{cases} \quad (19a)$$

$$\begin{cases} k_{1,i}^C < 1 \\ p_{23,i}^C = 0 \end{cases} \quad (19b)$$

From (19), the lower right block of (14) can be rewritten as

$$\begin{aligned} & [\mathcal{F}_{22,i}^C]^T \mathcal{P}_{22,i}^C + \mathcal{P}_{22,i}^C \mathcal{F}_{22,i}^C \\ &= \left[\frac{2 \frac{(k_{2,i}^C - R_{ti}^C)}{L_{ti}^C} p_{22,i}^C}{-p_{33,i}^C + \frac{k_{3,i}^C}{L_{ti}^C} p_{22,i}^C} \mid \frac{-p_{33,i}^C + \frac{k_{3,i}^C}{L_{ti}^C} p_{22,i}^C}{0} \right] \end{aligned} \quad (20)$$

Again based on Proposition 1, the off diagonal entities of (20) must be equal to zero which means

$$\frac{k_{3,i}^C}{L_{ti}^C} p_{22,i}^C = p_{33,i}^C \quad (21)$$

Furthermore, based on (19b), (21) and $P_i^C > 0$

$$k_{3,i}^C > 0 \quad (22)$$

Finally, for verifying $Q_i^C \neq 0$, one has

$$k_{2,i}^C < R_{ti}^C \quad (23)$$

Thus, P_i^C in (15) can be derived by substituting (19b) and (21) into (8) and then Q_i^C in (15) can be derived from (20) and (21), finally (19a), (23) and (22) consist of the set (16) for control coefficients. ■

An immediate consequence of Proposition 2 is the following results which will be exploited for proving the stability of the whole system through the LaSalle theorem.

Lemma 1: Let $g_i(w_i) = w_i^T Q_i^C w_i$. Under the Proposition 2, $\forall i \in \mathcal{D}^C$, only vectors \bar{w}_i in the form

$$\bar{w}_i = [\alpha_i \quad 0 \quad \beta_i]^T$$

with $\alpha_i, \beta_i \in \mathbb{R}$, fulfill

$$g_i(\bar{w}_i) = \bar{w}_i^T Q_i^C \bar{w}_i = 0. \quad (24)$$

Now the overall closed-loop model with multiple CDGUs is considered as

$$\begin{cases} \dot{\hat{\mathbf{x}}}^C(t) = (\hat{\mathbf{A}}^C + \hat{\mathbf{B}}^C \mathbf{K}^C) \hat{\mathbf{x}}^C(t) + \hat{\mathbf{M}}^C \hat{\mathbf{d}}^C(t) \\ \mathbf{z}^C(t) = \hat{\mathbf{H}}^C \hat{\mathbf{x}}^C(t) \end{cases} \quad (25)$$

obtained by combining (5) and (6), with $\mathbf{K}^C = \text{diag}(K_1^C, \dots, K_N^C)$. Also the collective Lyapunov function

$$\mathcal{V}^C(\hat{\mathbf{x}}^C) = \sum_{i=1}^N \mathcal{V}_i^C(\hat{x}_{[i]}^C) = [\hat{\mathbf{x}}^C]^T \mathbf{P}^C \hat{\mathbf{x}}^C \quad (26)$$

is considered, where $\mathbf{P}^C = \text{diag}(P_1^C, \dots, P_N^C)$.

One has $\dot{\mathcal{V}}^C(\hat{\mathbf{x}}^C) = [\hat{\mathbf{x}}^C]^T \mathbf{Q}^C \hat{\mathbf{x}}^C$ where

$$\mathbf{Q}^C = (\hat{\mathbf{A}}^C + \hat{\mathbf{B}}^C \mathbf{K}^C)^T \mathbf{P}^C + \mathbf{P}^C (\hat{\mathbf{A}}^C + \hat{\mathbf{B}}^C \mathbf{K}^C).$$

A consequence of Proposition 2 is that, the matrix \mathbf{Q}^C cannot be negative definite. At most, one has

$$\mathbf{Q}^C \leq 0. \quad (27)$$

Moreover, even if $Q_i^C \leq 0$ holds for all $i \in \mathcal{D}^C$, the inequality (27) might be violated because of the nonzero coupling terms \hat{A}_{ij}^C and load terms $\hat{A}_{load,i}^C$ in matrix $\hat{\mathbf{A}}^C$.

In order to derive that $Q_i^C \leq 0$ can guarantee (27), the following decomposition of matrix $\hat{\mathbf{A}}^C$ is considered

$$\hat{\mathbf{A}}^C = \hat{\mathbf{A}}_D^C + \hat{\mathbf{A}}_E^C + \hat{\mathbf{A}}_L^C + \hat{\mathbf{A}}_C^C, \quad (28)$$

where $\hat{\mathbf{A}}_D^C = \text{diag}(\hat{A}_{ii}^C, \dots, \hat{A}_{NN}^C)$ collects the local dynamics only, $\hat{\mathbf{A}}_C^C$ collects the coupling dynamic representing the off-diagonal items of matrix $\hat{\mathbf{A}}^C$, while $\hat{\mathbf{A}}_E^C = \text{diag}(\hat{A}_{\xi 1}^C, \dots, \hat{A}_{\xi N}^C)$ and $\hat{\mathbf{A}}_L^C = \text{diag}(\hat{A}_{load,1}^C, \dots, \hat{A}_{load,N}^C)$ with

$$\hat{A}_{\xi i}^C = \begin{bmatrix} -\sum_{j \in \mathcal{N}_i} \frac{1}{R_{ij} C_{ti}} & 0 & 0 \\ 0 & 0 & 0 \\ 0 & 0 & 0 \end{bmatrix}, \hat{A}_{load,i}^C = \begin{bmatrix} -\frac{1}{R_{Li} C_{ti}} & 0 & 0 \\ 0 & 0 & 0 \\ 0 & 0 & 0 \end{bmatrix}$$

represent the dependence of each local state on the neighboring CDGUs and the local resistive load. According to the decomposition (28), the inequality (27) is equivalent to

$$\underbrace{(\hat{\mathbf{A}}_D^C + \hat{\mathbf{B}}^C \mathbf{K}^C)^T \mathbf{P}^C + \mathbf{P}^C (\hat{\mathbf{A}}_D^C + \hat{\mathbf{B}}^C \mathbf{K}^C)}_{(a)} + \underbrace{2(\hat{\mathbf{A}}_E^C + \hat{\mathbf{A}}_L^C) \mathbf{P}^C}_{(b)} + \underbrace{(\hat{\mathbf{A}}_C^C)^T \mathbf{P}^C + \mathbf{P}^C \hat{\mathbf{A}}_C^C}_{(c)} \leq 0. \quad (29)$$

The next result shows that (27) can never be violated if (10) holds.

Proposition 3: If gains K_i^C are chosen according to (16), and (10) is fulfilled, then (27) holds.

Proof: For the proof of Proposition 3, we defer the reader to [16]. ■

Our next goal is to show asymptotic stability of the system with multiple CDGUs using the marginal stability result in Proposition 3 together with LaSalle invariance theorem. To this purpose, the main result is then given in Theorem 1 which relies on characterizing states $\hat{\mathbf{x}}^C$ deriving $\dot{\mathcal{V}}^C(\hat{\mathbf{x}}^C) = 0$.

Theorem 1: If (10) holds, and $Q_i^C \neq 0$ and the graph \mathcal{G}_{el} is connected and control coefficients are chosen according to (16), then the origin of (25) is asymptotically stable.

Proof: From Proposition 3, $\dot{\mathbf{V}}^C(\hat{\mathbf{x}}^C)$ is negative semidefinite meaning that (27) holds. We aim at showing that the origin of the system with multiple CDGUs is also attractive using the LaSalle invariance Theorem [18]. For this purpose, the set is computed $R^C = \{\mathbf{x}^C \in \mathbb{R}^{3N} : (\mathbf{x}^C)^T \mathbf{Q}^C \mathbf{x}^C = 0\}$ by means of the decomposition in (29), which coincides with

$$\begin{aligned} R^C &= \{\mathbf{x}^C : (\mathbf{x}^C)^T ((a) + (b) + (c)) \mathbf{x}^C = 0\} \\ &= \{\mathbf{x}^C : (\mathbf{x}^C)^T (a) \mathbf{x}^C + (\mathbf{x}^C)^T (b) \mathbf{x}^C + (\mathbf{x}^C)^T (c) \mathbf{x}^C = 0\} \\ &= \underbrace{\{\mathbf{x}^C : (\mathbf{x}^C)^T (a) \mathbf{x}^C = 0\}}_{X_1^C} \cap \underbrace{\{\mathbf{x}^C : (\mathbf{x}^C)^T [(b) + (c)] \mathbf{x}^C = 0\}}_{X_2^C} \end{aligned} \quad (30)$$

In particular, the last equality follows from the fact that (a) and (b)+(c) are negative semidefinite matrices (see the proof of Proposition 3).

First, based on Lemma 1, the set X_1^C is characterized as

$$X_1^C = \{\mathbf{x}^C : \mathbf{x}^C = [\alpha_1 \ 0 \ \beta_1 \mid \cdots \mid \alpha_N \ 0 \ \beta_N]^T, \alpha_i, \beta_i \in \mathbb{R}\} \quad (31)$$

Then, we focus on the elements of set X_2^C based on Proposition 3. Since matrix (b) + (c) can be seen as an "expansion" of a matrix which is negative definite matrix with zero entries on the second and third rows and columns of 3×3 block, by construction, vectors in the form

$$X_2^C = \{\mathbf{x}^C : \mathbf{x}^C = [0 \ \tilde{x}_{12} \ \tilde{x}_{13} \mid \cdots \mid 0 \ \tilde{x}_{N2} \ \tilde{x}_{N3}]^T, \tilde{x}_{i2}, \tilde{x}_{i3} \in \mathbb{R}\} \quad (32)$$

Hence, by merging (31) and (32), and from (30), it derives that

$$R^C = \{\mathbf{x} : \mathbf{x} = [0 \ 0 \ \beta_1 \mid \cdots \mid 0 \ 0 \ \beta_N]^T, \beta_i \in \mathbb{R}\} \quad (33)$$

Finally, in order to conclude the proof, it should be shown that the largest invariant set $M^C \subseteq R$ is the origin. To this purpose, (11) is considered, by adding the coupling terms $\hat{\xi}_{[i]}$ and the resistive load term $\hat{A}_{load,i}^C \hat{x}_i^C(0)$, setting load disturbance $\hat{d}_{[i]}^C = 0$, choosing the initial state $\hat{\mathbf{x}}^C(0) = [\hat{x}_1^C(0) \mid \cdots \mid \hat{x}_N^C(0)]^T \in R^C$. In order to find conditions on the elements of $\hat{\mathbf{x}}^C(0)$ that must hold for having $\dot{\hat{\mathbf{x}}}^C \in R^C$, one has

$$\begin{aligned} \dot{\hat{x}}_i^C(0) &= F_i^C \hat{x}_i^C(0) + \hat{A}_{load,i}^C \hat{x}_i^C(0) + \underbrace{\sum_{j \in \mathcal{N}_i} \hat{A}_{ij}^C (\hat{x}_j^C(0) - \hat{x}_i^C(0))}_{=0} \\ &= \begin{bmatrix} -\frac{1}{R_{Li} C_{ti}} & \frac{1}{C_{ti}} & 0 \\ \frac{k_{1,i}^C - 1}{L_{ti}^C} & \frac{k_{2,i}^C - R_{ti}^C}{L_{ti}^C} & \frac{k_{3,i}^C}{L_{ti}^C} \\ 0 & -1 & 0 \end{bmatrix} \begin{bmatrix} 0 \\ 0 \\ \beta_i \end{bmatrix} \\ &= \begin{bmatrix} 0 \\ \frac{k_{3,i}^C}{L_{ti}^C} \beta_i \\ 0 \end{bmatrix} \end{aligned}$$

for all $i \in \mathcal{D}^C$. It follows that $\dot{\hat{\mathbf{x}}}^C(0) \in R$ only if $\beta_i = 0$. Since $M^C \subseteq R$, from (33) one has $M^C = \{0\}$. ■

Remark 3: The design of stabilizing controller for each CDGU can be conducted according to (16) in Proposition 2.

In particular, differently from the approach in [7], no optimization problem has to be solved for stabilizing controllers. Indeed, it is enough to choose control coefficient $k_{1,i}^C$, $k_{2,i}^C$ and $k_{3,i}^C$ from inequality set (16). Note that these inequalities are always feasible, implying that a stabilizing controller always exists. Moreover, the inequalities depend only on the parameter R_{ti}^C of the CDGU i . Therefore, the control synthesis is independent of parameters of CDGUs and power lines which means that controller design can be executed only once for each CDGU in a plug-and-play fashion. From Theorem 1, local controllers also guarantee stability of the whole MG. When new CDGUs are plugged in the MG, their controller are designed as described above, the connectivity of the electrical graph \mathcal{G}_{el} is preserved and have Theorem 1 applied to the whole MG. Instead, when a CDGU is plugged out, the electrical graph \mathcal{G}_{el} might be disconnected and split into two connected graphs. Theorem 1 can still be applied to show the stability of each sub-MG.

IV. HARDWARE-IN-LOOP TESTS

To verify the effectiveness of proposed controller, real-time HiL tests are carried out based on dSPACE 1006. By this way, the time span in the simulation is equals to that in real system. The real-time simulation model is comprised of four CDGUs with meshed topology as shown in Fig. 2. The electrical parameters and control coefficients for each CDGU are shown in Table I, and the transmission line parameters are shown in Appendix B of [16].

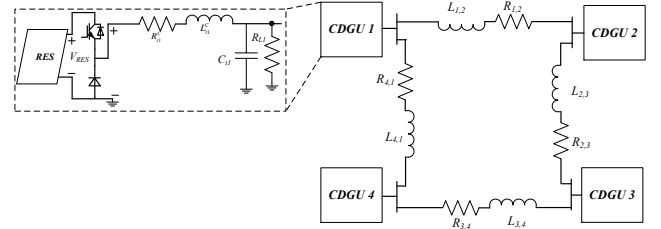


Fig. 2: System Configuration of Hardware-in-Loop Test.

TABLE I: Electrical setup parameters and Control coefficients

Parameters	Symbol	Value
Output capacitance	C_{t*}	2.2 mF
Inductance for CDGU	L_{t*}^C	0.018 H
Inductor + switch loss resistance for CDGU	R_{t*}^C	0.2 Ω
Switching frequency	f_{sw}	10 kHz
Control Coefficients	$k_{1,*}^C$	-0.01
	$k_{2,*}^C$	-2.7015
	$k_{3,*}^C$	40.4018

Each CDGU is started separately with different current reference. Meanwhile, the voltages at PCC point are supported by different voltage values which are 47.8V, 47.9V, 48V, 48.2V for CDGUs 1 – 4. For CDGUs 1 – 4, the current references are 1A, 2A, 3A, 4A. At T1, four CDGUs are connected together simultaneously. As shown in Fig. 3b, the output current can still follow the local references without

oscillations. At T_2 , the current reference for CDGU 1 is changed from 1A to 2.5A. At T_3 , the current reference for CDGU 2 is changed from 2A to 3.5A. At T_4 , the current reference for CDGU 3 is changed from 3A to 4.5A. At T_5 , the current reference for CDGU 4 is changed from 4A to 5.5A. As shown in Fig. 3b, the output currents can track the changed reference. In addition, as shown in Fig. 3a, when the current references are changed, the PCC voltages are only affected by little oscillations (approximately 0.05V) which means the CDGUs cannot affect the voltage stability in the system. Furthermore, At T_6 , CDGU 2 is plugged out of the system and operated separately. Then at T_7 , CDGU 2 is plugged in the system. As shown in Fig. 3, the system can operate stable which illustrates the PnP effectiveness of proposed controller.

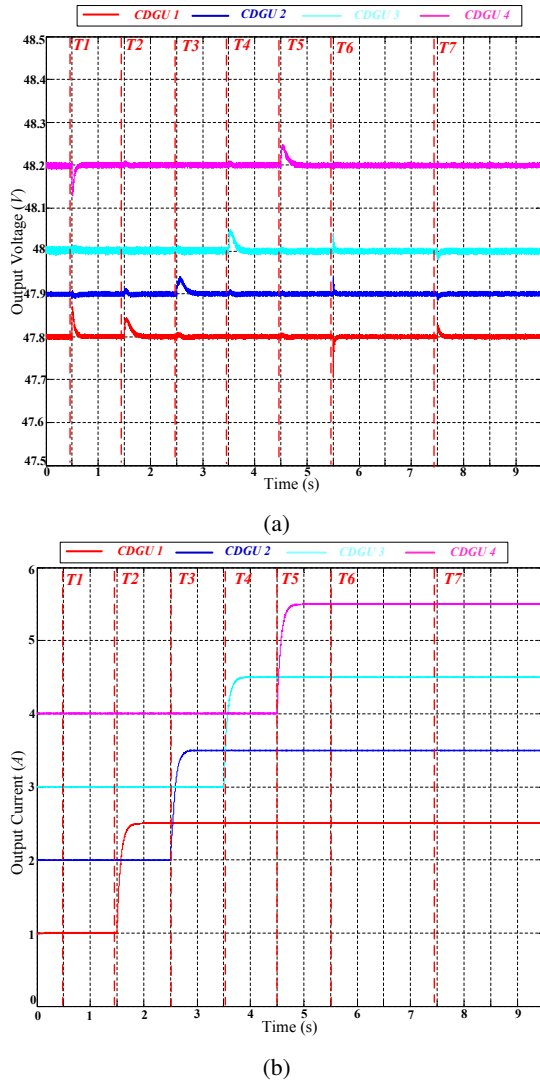


Fig. 3: Current Tracking and PnP Test: (a). Voltage Performance; (b). Current Performance.

V. CONCLUSIONS

The inequality set for control coefficients is found for the proposed current PnP controller which can guarantee the

stability of the whole system achieving seamless plug-in/out operation. In the paper, it is assumed that the voltage at PCC point has already been supported. Actually, the stability proof considering both the voltage support and current feeding simultaneously are included in the technical report [16]. By applying the inequality set as the constraints, the control performance can be further optimized by the optimization algorithms.

REFERENCES

- [1] N. Hatziaargyriou, H. Asano, R. Iravani, and C. Marnay, "Microgrids," *Power and Energy Magazine, IEEE*, vol. 5, no. 4, pp. 78–94, July 2007.
- [2] J. Rocabert, A. Luna, F. Blaabjerg, and P. Rodriguez, "Control of power converters in ac microgrids," *IEEE Transactions on Power Electronics*, vol. 27, no. 11, pp. 4734–4749, Nov 2012.
- [3] T. Dragičević, X. Lu, J. Vasquez, and J. Guerrero, "DC microgrids—part I: A review of control strategies and stabilization techniques," *IEEE Transactions on Power Electronics*, vol. 31, no. 7, pp. 4876–4891, 2016.
- [4] C. De Persis, E. Weitenberg, and F. Dörfler, "A power consensus algorithm for dc microgrids," *arXiv preprint arXiv:1611.04192*, 2016.
- [5] J. M. Guerrero, J. C. Vasquez, J. Matas, D. Vicuna, L. Garcia, and M. Castilla, "Hierarchical control of droop-controlled AC and DC microgrids - A general approach toward standardization," *IEEE Transactions on Industrial Electronics*, vol. 58, no. 1, pp. 158–172, 2011.
- [6] M. Tucci, S. Rivero, J. C. Vasquez, J. M. Guerrero, and G. Ferrari-Trecate, "A decentralized scalable approach to voltage control of dc islanded microgrids," *IEEE Transactions on Control Systems Technology*, vol. 24, no. 6, pp. 1965–1979, Nov 2016.
- [7] M. Tucci, S. Rivero, and G. Ferrari-Trecate, "Line-independent plug-and-play controllers for voltage stabilization in dc microgrids," *IEEE Transactions on Control Systems Technology*, vol. PP, no. 99, pp. 1–9, 2017.
- [8] H. Wang, M. Han, R. Han, J. Guerrero, and J. Vasquez, "A decentralized current-sharing controller endows fast transient response to parallel dc-dc converters," *IEEE Transactions on Power Electronics*, vol. PP, no. 99, pp. 1–1, 2017.
- [9] Q. Shafiee, T. Dragičević, J. C. Vasquez, and J. M. Guerrero, "Hierarchical Control for Multiple DC-Microgrids Clusters," *IEEE Transactions on Energy Conversion*, vol. 29, no. 4, pp. 922–933, 2014.
- [10] V. Nasirian, S. Moayedi, A. Davoudi, and F. L. Lewis, "Distributed cooperative control of dc microgrids," *IEEE Transactions on Power Electronics*, vol. 30, no. 4, pp. 2288–2303, April 2015.
- [11] J. Zhao and F. Dörfler, "Distributed control and optimization in DC microgrids," *Automatica*, vol. 61, pp. 18–26, 2015.
- [12] D. Wu, F. Tang, T. Dragicevic, J. M. Guerrero, and J. C. Vasquez, "Coordinated control based on bus-signaling and virtual inertia for islanded dc microgrids," *IEEE Transactions on Smart Grid*, vol. 6, no. 6, pp. 2627–2638, Nov 2015.
- [13] X. Zhao, Y. W. Li, H. Tian, and X. Wu, "Energy management strategy of multiple supercapacitors in a dc microgrid using adaptive virtual impedance," *IEEE Journal of Emerging and Selected Topics in Power Electronics*, vol. 4, no. 4, pp. 1174–1185, Dec 2016.
- [14] T. Dragicevic, J. M. Guerrero, J. C. Vasquez, and D. Skrlec, "Supervisory control of an adaptive-droop regulated DC microgrid with battery management capability," *IEEE Transactions on Power Electronics*, vol. 29, no. 2, pp. 695–706, Feb 2014.
- [15] R. Han, N. L. D. Aldana, L. Meng, J. M. Guerrero, and Q. Sun, "Droop-free distributed control with event-triggered communication in dc micro-grid," in *2017 IEEE Applied Power Electronics Conference and Exposition (APEC)*, March 2017, pp. 1160–1166.
- [16] R. Han, M. Tucci, R. Soloperto, A. Martinelli, G. Ferrari-Trecate, and J. M. Guerrero, "Hierarchical Plug-and-Play Voltage/Current Controller of DC microgrid with Grid-Forming/Feeding modules: Line-independent Primary Stabilization and Leader-based Distributed Secondary Regulation," *ArXiv e-prints*, July 2017.
- [17] S. Skogestad and I. Postlethwaite, *Multivariable feedback control: analysis and design*. New York, NY, USA: John Wiley & Sons, 1996.
- [18] H. K. Khalil, *Nonlinear systems (3rd edition)*. Prentice Hall, 2001.